Journal of Functionally Graded Materials Vol.33, 16-22 (2019)

Original paper

Strength improvement of poly(vinyl alcohol) (PVA) reinforced by Halloysite nanotube (HNT) treated with sulfuric acid

Antonio Norio Nakagaito[1)], Kohei Fujii[2)], Hitoshi Takagi[3)], and Yu Dong[4)]
1) Institute of Technology and Science, Tokushima University, Tokushima 770-8506, Japan, E-mail: nakagaito@tokushima-u.ac.jp
2) Graduate School of Advanced Technology and Science, Tokushima University, Tokushima 770-8506, Japan, E-mail: k0uhei238@yahoo.co.jp
3) Institute of Technology and Science, Tokushima University, Tokushima 770-8506, Japan, E-mail: takagi@tokushima-u.ac.jp
4) Department of Civil and Mechanical Engineering, Curtin University, Perth WA 6845, Australia, E-mail: Y.Dong@curtin.edu.au

Abstract Halloysite nanotube (HNT) is a natural clay mineral with a hollow and tubular structure, which can be a potential reinforcement for biodegradable polymers such as poly(vinyl alcohol) (PVA). This study investigates the improvement of interfacial adhesion between HNT and PVA by means of controlled acid etching on HNT surfaces. Such an improvement is attributed to a porous structure with rough HNT surfaces in that acid favors the dissolution of AlO_6. The strength of PVA/HNT nanocomposites increased up to 10% when HNT were subjected to 1 h acid treatment. However, the reinforcement effect could have been more pronounced if HNT aspect ratio were maintained during the composite fabrication process.
Key words: halloysite, clay, poly(vinyl alcohol), acid, etching

1. INTRODUCTION

Halloysite is an aluminosilicate clay mineral, which belongs to the kaolin family. The material consists of tiny hollow tubular structures with a large aspect ratio, which explains the more common designation halloysite nanotube (HNT). The typical HNT dimensions are 1 – 30 nm and 30 – 50 nm for internal and external diameters, respectively, along with lengths in the range of 100 – 200 nm [1)]. It also exhibits high functionality, good biocompatibility, and high mechanical strength [2)]. Its density, owing to the hollow structure, is much lower than other mineral fillers like talc and calcite while the elastic modulus of HNT is 140 GPa [3)], a value close to that of aramid. In addition, HNT does away with the requirements of exfoliation and intercalation required by other nanoclays such as montmorillonites to achieve homogeneous dispersion within polymer matrices [4)]. There are numerous applications based on HNT such as raw material for porcelain tableware, controlled release capsules filled with additives in paints and sealants, lubricants, herbicides, cosmetics, drugs, etc. [5)] The HNT is an inexpensive alternative nanofiller to multiwalled carbon nanotube owing to their similar tubular structures when used as reinforcements in composite materials. The HNT has an ideal chemical formula of $Al_2Si_2O_5(OH)_4 \cdot nH_2O$. When n = 2, there is a layer of water molecules that fill interlayer spaces. Hence such a hydrated state is called halloysite-(10 Å). When n = 0, the water layer is lost by drying, resulting in an irreversible fully dehydrated state known as halloysite-(7 Å) [5)]. Their crystal structure consists of two layers made of a corner-sharing SiO_4 tetrahedral layer and an edge-sharing AlO_6 octahedral layer. These layers may be intercalated by a monomolecular layer of water in a hydrated state [2)].

Although HNT was subjected to extensive research in the 1940's, there is again a renewed interest that has been intensified in recent years [3)]. The use of HNT as filler in composites has been considered in several polymeric matrices such as epoxies [6-12)], polyamides [13-15)], polypropylene [16-22)], starch [23-26)], poly(vinyl alcohol) (PVA) [27-29)], with positive results obtained especially in terms of fracture toughness and thermal stability. It is also used as filler in poly(lactic acid) (PLA) nanofibers obtained by electrospinning [30-33)]. Among these polymeric matrices, PVA has some interesting material characteristics. It is an odorless, tasteless petroleum-based synthetic polymer mainly used as adhesives and binders, and can be completely biodegradable under certain conditions. PVA is produced by the polymerization of vinyl acetate, of which ester groups are later partially replaced with hydroxyl groups by using the hydrolysis process. Due to hydroxyl groups on the repeating polymeric units, PVA is hydrophilic and also soluble in water. However, similar to many other polymers, the

relatively low strength of PVA requires certain reinforcement to suit more mechanically demanding applications. For a biodegradable polymer, the reinforcing phase is also expected to have equally low impact on the environment. Therefore, PVA and HNT were selected to produce nanocomposites owing to their environmental friendliness and much lower cost than the materials employed in conventional composites. In order to improve the PVA-HNT interfacial adhesion, a simple sulfuric acid treatment of HNT was undertaken to investigate its effect on the mechanical properties of resulting nanocomposites. The roughness of HNT surface was anticipated to be obtained according to previous literature [2], in which sulfuric acid dissolved the AlO_6 octahedral layers and increased porosity of HNT, so that its physico-chemical characteristics required as adsorbents could be evaluated. Our initial study confirmed the improvement of HNT-matrix adhesion via an acid etching on HNT surfaces [34].

The objective of this study was to evaluate the effect of acid treatment of HNTs on the mechanical properties of PVA/HNT nanocomposites. The surface modification was achieved by a 1 h-acid treatment that produced a composite strength enhancement of about 10% over the untreated HNT reinforcement. Such an acid treatment may shed light on the reinforcement of other polymers by HNT, as a low cost and effective surface modification method.

2. EXPERIMENTAL

2.1 Materials

The HNT powder used in this study was kindly donated by Imerys Tableware Asia Ltd., New Zealand. Polyvinyl alcohol EXCEVAL RS-2817 (degree of hydrolysis: 95.5-97.5 mol%) was provided by Kuraray Co., Ltd., Japan and the sulfuric acid was purchased from Wako Chemical Industries, Ltd., Japan. Halloysite (685445) as reference reinforcing material was purchased from Sigma-Aldrich.

2.2 Sulfuric acid treatment of HNT

The treatments were performed at an acid concentration of 3 mol L^{-1}. First, 8 g of HNT powder was mixed in 83.5 ml of distilled water and sonicated in an ultrasonic bath for 1 hour. Subsequently, 16.5 mL of 97% purity sulfuric acid was dripped to the suspension, further stirring and maintaining the temperature at 80°C in an oil bath for different treatment times (1, 2, 4, and 8 h). After the acid treatment, the suspensions were alternately vacuum-filtered and washed in distilled water several times, until the pH became 7. Finally, the acid-treated HNT was oven-dried at 105°C for 20 min. and crushed back into powder by a mortar and pestle.

2.3 Nanocomposite film preparation

A 3 wt% PVA aqueous solution was initially prepared by completely diluting 15 g of PVA powder into 485 mL of distilled water at 80°C. Subsequently, 1 g of HNT powder was mixed in 150 mL of distilled water in a beaker and kept in an ultrasonic bath at 24 kHz and 31 kHz in an alternating mode for 1 h. The suspension remained still for 24 h to allow agglomerated particles to precipitate. Only the supernatant portion with individualized waterborne HNT particles was collected. The HNT concentration was calculated from the mass difference of precipitated and initial HNT. The PVA solution and HNT supernatant suspension were mixed by controlling the HNT amounts in order to obtain the desired HNT content in the final PVA/HNT nanocomposites. The mixture was stirred in vacuum to eliminate air bubbles entrapped in the aqueous suspension. The suspension was poured into a plastic tray with flat bottom and films were cast in a convection oven at a temperature of 40°C for 5 days. Thin nanocomposite films with the HNT contents of 2, 4, 6, and 8 wt% were obtained accordingly.

2.4 Tensile test

Ribbon-like testing specimens in sizes of 50 mm × 10 mm were cut from the nanocomposite films, based on which tensile tests were carried out using an Instron 5567 universal testing machine (Instron Corporation, USA) at a crosshead speed of 1.0 mm min^{-1}. The gage length was set at 30 mm for all specimens. To prevent any damage at the gripping areas, each specimen ends were glued with thick paper tabs and clasped using serrated chucks. The thickness and width were measured at 6 different equidistant positions along the gage length of each specimen. The cross sectional areas corresponding to the actual fracture sites were used to calculate the Young's modulus and tensile strength. The measured values were based on the average of at least 5 replicates.

2.5 Scanning electron microscopy (SEM)

Fracture surfaces of nanocomposites after tensile test were examined using a field emission scanning electron microscope, model S-4700 (Hitachi High-Technologies Corporation, Japan). The accelerating voltage was set to 3 kV, and samples were coated with platinum to avoid specimen charging.

2.6 Energy-dispersive X-ray spectroscopy (EDS)

Elemental analysis was performed in a scanning electron microscope model JSM-6510A (JEOL Ltd., Japan) with an accelerating voltage of 5 kV, spot size 65, and aperture of 100 μm in diameter.

2.7 Transmission electron microscopy (TEM)

Observations of HNT structure before and after acid treatment were performed by a transmission electron microscope model JEM-2100F (JEOL Ltd., Japan). Specimens were prepared by dripping aqueous suspensions containing HNT on

copper meshes and let them dry at ambient temperature.

2.8 Fourier transform infra-red spectroscopy (FTIR)

The measurements by FTIR were carried out at room temperature using a Bio-Rad FTS 3000MX FTIR spectrometer (Varian Inc., USA) in the spectral range of 3,200 to 4,000 cm^{-1}.

2.9 Optical transmittance

The light transmittances of nanocomposite films were detected at a wavelength range from 200 to 800 nm by a UV-visible spectrophotometer model V-570 (JASCO Co., Japan).

2.10 HNT aspect ratio measurement

The aspect ratio distribution of HNT particles was determined by visual inspection and image measurement obtained by SEM. A hundred individual HNTs were chosen at random and their diameters and lengths were manually measured using a graduated scale. Aspect ratios were determined by dividing the length of each particle by its respective diameter.

3. RESULTS AND DISCUSSION

The aspect ratio of reinforcing elements has a significant effect on the mechanical properties of resulting nanocomposites. The calculated aspect ratio distribution of HNTs used in this study is depicted in Fig. 1. These results are based on the morphological comparison of two different types of HNTs received from Sigma-Aldrich and Imerys Tableware. The average aspect ratio of HNT from Imerys was found to be slightly larger than that from Sigma-Aldrich. Apparently the latter have a broad diameter distribution but with quite shorter lengths compared to the former.

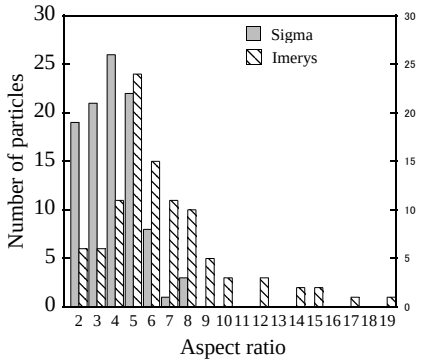

Fig. 1 Aspect ratio distribution of HNTs from two different sources (Sigma-Aldrich and Imerys Tableware).

To establish the relationship between aspect ratio of fillers and reinforcement effect, untreated HNT-reinforced PVA nanocomposites based on these two different types of HNTs were fabricated, and their tensile properties measured. The tensile strengths and moduli of PVA/HNT nanocomposites as a function of HNT content are shown in Figs. 2a and 2b, respectively. Overall, the HNT morphology with a higher aspect ratio resulted in better mechanical properties of nanocomposites, as expected. There was a slight increase in strength with increasing HNT content, practically levelling off, but decreased at 8 wt%, probably caused by the HNT agglomerations at high filler contents. The difference for HNT dispersion in PVA matrices is shown by SEM micrographs of fractured surfaces in Figs. 3a and 3b. At a HNT content of 6 wt% (Fig. 3a), the surface becomes quite homogeneous while at a higher content level of 8 wt%, there are visible portions of clustered HNTs. Accordingly, HNT with a larger aspect ratio (Imerys) was chosen, and its content was fixed at 6 wt% in order to evaluate the effect of acid treatment of HNT on the mechanical properties of PVA/HNT nanocomposites.

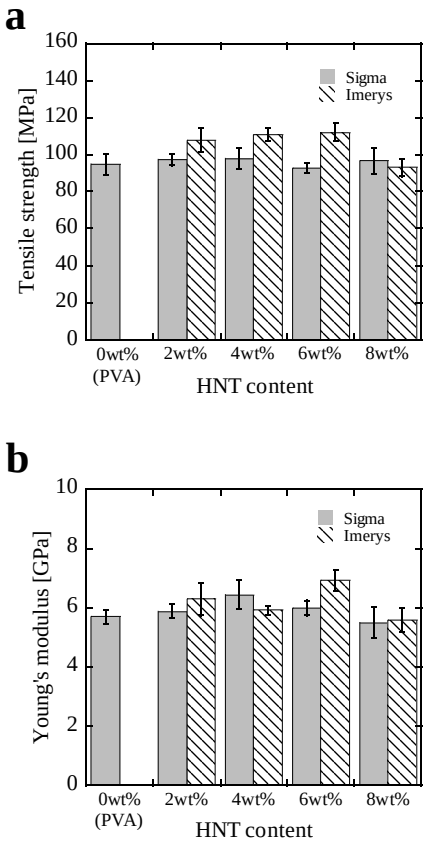

Fig. 2 Tensile properties of untreated HNT-reinforced PVA nanocomposites as a function of the HNT content: a. Tensile strength at yield; b. Young's modulus.

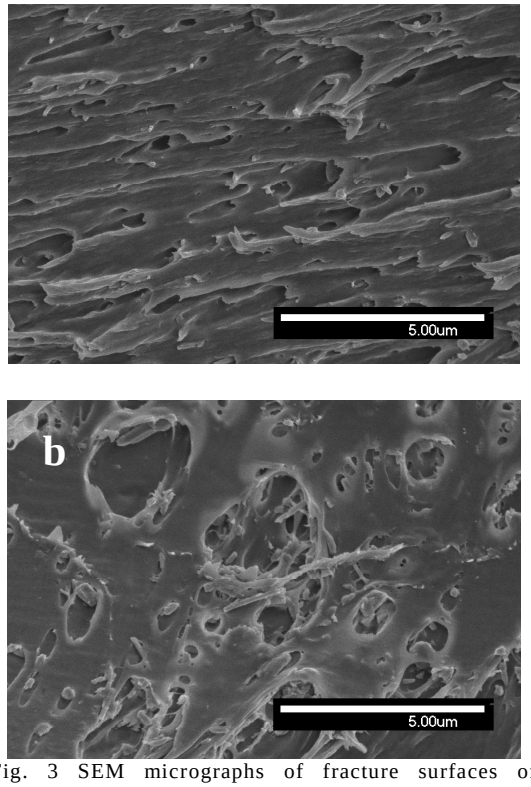

Fig. 3 SEM micrographs of fracture surfaces of untreated HNT-reinforced PVA nanocomposites with two typical HNT contents: a. 6 wt% and b. 8 wt%.

The sulfuric acid treatment was intended to enhance the roughness of HNT surface and thus increase the PVA-HNT interfacial adhesion. Sulfuric acid tends to preferentially dissolve AlO_6 octahedral layers of the HNT structure [2]. As seen in the FT-IR spectra in Fig. 4, HNT shows two intense peaks at 3696 cm^{-1} corresponding to silanol (Si-OH) and at 3618 cm^{-1} related to interlayer hydroxyl groups. Compared with the spectrum of untreated HNT, as the acid treatment time increases, the silanol peak becomes more intense relative to the hydroxyl peak. This can be ascribed to the removal of hydroxyl groups in AlO_6 octahedral layer with dissolving Al^{3+} as reported by Zhang et al. [2] Elemental analysis results shown in Fig. 5, confirm that the Si to Al atomic ratio increased linearly with the acid treatment time in that the Al was removed by the acid dissolution.

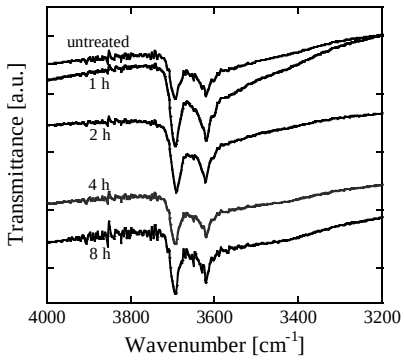

Fig. 4: FTIR spectra of untreated and sulfuric acid-treated HNTs (labeled values correspond to sulfuric acid treatment times).

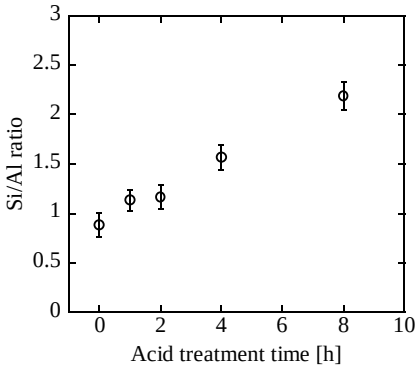

Fig. 5 Silicon to aluminum ratio as a function of HNT acid treatment time obtained from elemental analysis.

The crystal structures of untreated and acid-treated HNTs were characterized by X-ray diffraction (XRD). Figure 6 shows that all diffractograms have a sharp peak at 2θ around 12.4°, corresponding to the (001) reflection plane of dehydrated halloysite-(7 Å). The absence of a peak at about 9° indicates that the amount of hydrated halloysite-(10 Å) is too small to be detected by XRD. The acid treatment appears not to change these peaks significantly, indicating that the crystallinity is somehow kept in the range of treatment time up to 8 h. A broad peak at 2θ values between 15° and 35°, corresponding to amorphous silica as described by Zhang et al. [2] for sulfuric acid treatments above 3 h, was not evident in the present study. This phenomenon signifies that the crystallinity mostly remains after acid treatments.

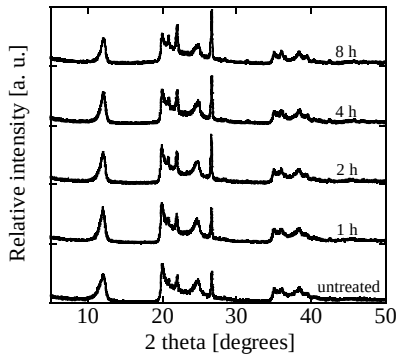

Fig. 6 X-ray diffractograms of untreated and sulfuric acid-treated HNTs (labeled values correspond to sulfuric acid treatment times).

In addition, the effect of acid treatment of HNT on the mechanical properties of PVA/HNT nanocomposites was evaluated. Figures 7a and 7b show the tensile strengths and moduli of nanocomposite films, respectively, as a function of the acid treatment time of HNT. Acid treatment of HNT increased the strength of nanocomposites relative to untreated HNT, with the best performance being achieved by a 1 h treatment. However, the gain in strength was modest and the tensile modulus decreased for PVA/acid-treated HNT nanocomposites. Mechanical crushing of treated HNTs with a mortar and pestle was the only significant difference between untreated and acid-treated nanofiller handling procedures. After acid-treatment and rinsing, HNTs formed aggregates upon drying, which made it necessary to return them to the powder form. The crushing step may have shortened the size of HNT, therefore the aspect ratios of untreated and acid-treated materials were evaluated. The associated results are illustrated in Fig. 8. The aspect ratio distribution demonstrates that the average aspect ratio was reduced to a lower value after the acid treatment, and it possibly happened during the crushing processing of HNT agglomerates into powder. It means that if the mechanical action is replaced by a less destructive process for disaggregation (e.g. sonication) or even eliminating the drying step, a better reinforcement effect can be obtained by the acid treatment. Even so, the reinforcing trend is clear and a sulfuric acid treatment for 1 h appears to be close to the optimum condition for this purpose.

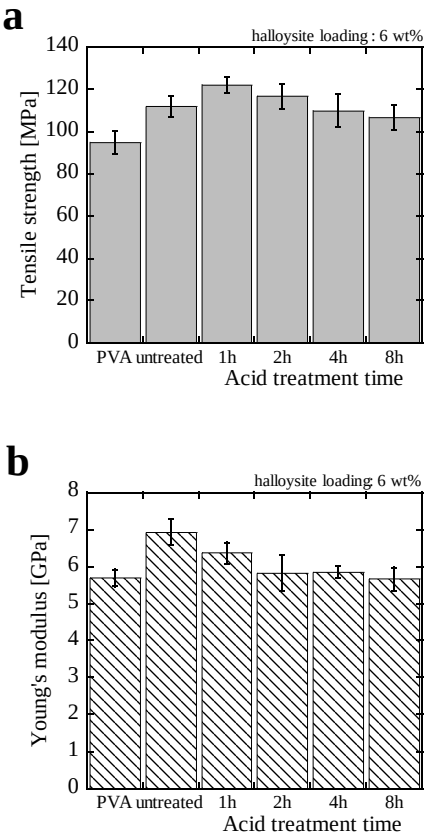

Fig. 7 Tensile properties of PVA/HNT nanocomposites as a function of HNT acid treatment time: a. Tensile strength at yield; b. Young's modulus.

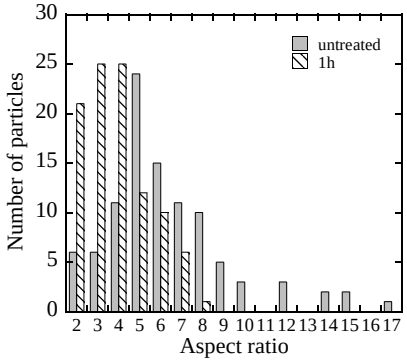

Fig. 8 Aspect ratio distribution of HNTs before (untreated) and after acid-treatment for 1 h (subjected to mortar and pestle crushing).

The TEM micrographs of untreated and acid-treated HNT for 1 and 8 h (dried from aqueous suspensions) are presented in Figs. 9a-c. There are no visible differences between the untreated and 1 h-treated HNTs. However, judging from the highly porous 8 h-acid treated HNT, it can be concluded that the acid treatment causes a gradual increase in the porosity of HNT walls and consequent roughness that contributes to a better interfacial adhesion with PVA matrices

in nanocomposites. However, when the treatment time was extended further, the increase in roughness was accompanied by a weakened HNT structure owing to the dissolution of the AlO_6 portion. As a result, a short 1 h treatment led to an optimum balance of surface roughness and tensile strength of nanocomposites.

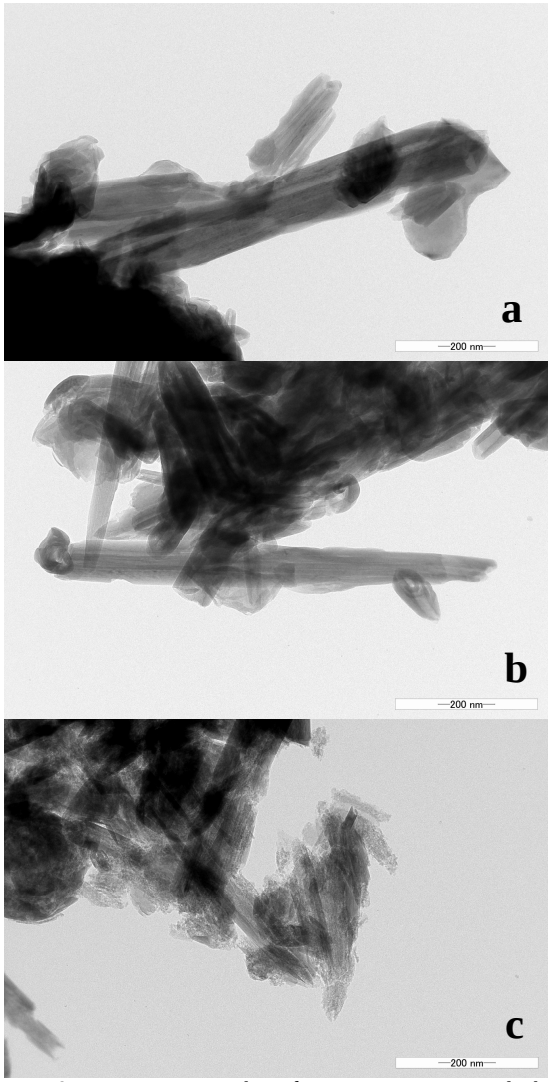

Fig. 9 TEM micrographs of HNTs: a. untreated; b. sulfuric acid-treated for 1 h; c. sulfuric acid-treated for 8 h.

The Young's modulus of composites, however, decreased with acid treatment of halloysite. Even though the porosity and consequent surface roughness of halloysite contributed to the increase in the composite's strength, the dissolution of AlO_6 layers might have resulted in a porous but less rigid crystalline structure constituted by the remaining SiO_4 layers. In this study, while the untreated halloysite reinforcement increased the Young's modulus, a 1 h-acid treatment resulted in a conspicuous fall in the composite modulus. Longer acid treatments resulted in no increase whatsoever in modulus over the neat PVA matrix. The acid treatment of halloysite led to the reduction of the composites stiffness.

Apart from the promising reinforcing-phase role of HNT in nanocomposites, they can also produce optically transparent composite materials. Due to the nanosized dimension that is much smaller than the visible light wavelength, the light scattering can be minimized if the particles are evenly dispersed into transparent matrices [35]. Figure 10 shows the light transmittance of PVA and PVA/HNT nanocomposites as a function of the wavelength. The PVA/acid-treated HNT nanocomposites have the transmittance lower than neat PVA, but higher than PVA/untreated HNT nanocomposites. The transmittance gradually decreased as the acid treatment time increased, which is possibly associated with the interfaces between HNT and PVA. As implied by the high tensile strength of nanocomposites with the best adherence for 1 h-treated HNTs, the light scattering at interfaces can be minimized. Longer treatment time gives rise to less bonded interfaces with more scattering. Another possibility is that the differences in the HNT density caused by acid treatment result in larger mismatches of refractive index with PVA matrices, thus increasing light scattering.

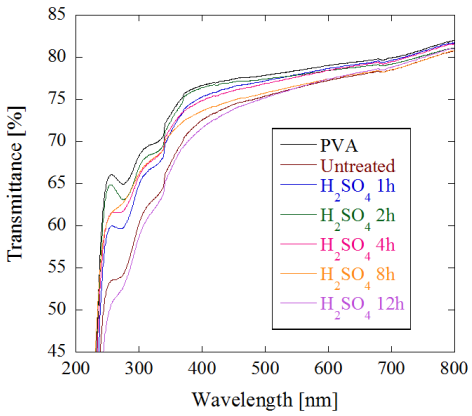

Fig. 10 Optical transmittance of PVA and PVA/HNT composite films as a function of wavelength.

The PVA nanocomposites reinforced with 1 h acid-treated HNTs had similar transparency to that of neat PVA, especially at shorter wavelengths. It is expected that the control of HNT acid treatment would facilitate achieving more effective reinforcement of nanofillers with improved transparency.

4. CONCLUSIONS

Sulfuric acid-treatment of HNT was performed aiming to increase the interfacial adhesion with PVA matrices. A treatment time of 1 hour was found to achieve effective reinforcement effect of PVA/HNT nanocomposites with a tensile strength increase of about 10% over corresponding nanocomposites reinforced with untreated HNT. The mechanical properties of acid-treated HNT nanocomposites might be more significant if the crushing step after acid-treatment, to eliminate

the HNT aggregation caused by drying, were removed. Mechanical crushing could cause the reduction in the HNT aspect ratio, limiting the reinforcing capability of nanofillers.

ACKNOWLEDGMENTS

We thank Imerys Tableware Asia Ltd., New Zealand for providing the HNT and Kuraray Co. Ltd. for furnishing the PVA sample used in this study. We are also grateful to Associate Professor M. Katoh from the Department of Chemical Science and Technology, Tokushima University for FTIR measurements and related discussions, and Professor D. Yonekura and Associate Professor K. Kusaka from the Department of Mechanical Engineering, Tokushima University for the support in UV-vis. spectroscopy and XRD, respectively. Appreciation is extended to Mr. T. Ueki from the Institute of Technology and Science, Tokushima University for the TEM and elemental analysis measurements.

REFERENCES

1) M. L. Du, B. C. Guo and D. M. Jia, Polymer International 59 (2010), 574-582
2) A. B. Zhang, L. Pan, H. Y. Zhang, S. T. Liu, Y. Ye, M. S. Xia and X. G. Chen, Colloid Surface A 396 (2012), 182-188
3) M. X. Liu, Z. X. Jia, D. M. Jia and C. R. Zhou, Progress in Polymer Science 39(2014), 1498-1525
4) S. Q. Deng, J. N. Zhang and L. Ye, Composites Science and Technology 69 (2009), 2497-2505
5) E. Joussein, S. Petit, J. Churchman, B. Theng, D. Righi and B. Delvaux, Clay Minerals 40 (2005), 383-426
6) Y. P. Ye, H. B. Chen, J. S. Wu and C. M. Chan, Composites Part B-Engineering 42(2011), 2145-2150
7) Y. H. Tang, S. Q. Deng, L. Ye, C. Yang, Q. A. Yuan, J. N. Zhang and C. B. Zhao, Composites Part A-Applied Science and Manufacturing 42 (2011), 345-354
8) M. X. Liu, B. C. Guo, M. L. Du, X. J. Cai and D. M. Jia, Nanotechnology 18 (2007) Article number 455703
9) M. X. Liu, B. C. Guo, M. L. Du, Y. D. Lei and D. M. Jia, Journal of Polymer Research 15(2008), 205-212
10) I. Legocka, E. Wierzbicka, T. J. M. Al-Zahari and O. Osawaru, Polish Journal of Chemical Technology 13 (2011), 47-52
11) S. Q. Deng, J. N. Zhang, L. Ye and J. S. Wu, Polymer 49 (2008), 5119-5127
12) R. Nakamura, A. N. Netravali and M. V. Hosur, Journal of Adhesion Science and Technology 26 (2012), 1295-1312
13) K. Prashantha, M. F. Lacrampe and P. Krawczak, Journal of Applied Polymer Science 130) (2013), 313-321
14) K. Prashantha, H. Schmitt, M. F. Lacrampe and P. Krawczak, Composites Science and Technology 71 (2011), 1859-1866
15) I. Legocka, E. Wierzbicka, T. M. J. Al-Zahari and O. Osawaru, Polimery 58 (2013), 24-32
16) K. Prashantha, M. F. Lacrampe and P. Krawczak, Express Polymer Letters 5(2011), 295-307
17) K. Prashantha, J. Soulestin, M. F. Lacrampe and P. Krawczak, International Journal of Polymer Analysis and Characterization 19 (2014), 363-371
18) M. X. Liu, B. C. Guo, M. L. Du, F. Chen and D. M. Jia, Polymer 50(2009), 3022-3030
19) M. X. Liu, B. C. Guo, M. L. Du and D. M. Jia, Polymer Journal 40(2008), 1087-1093
20) M. X. Liu, B. C. Guo, M. L. Du, Q. L. Zou and D. M. Jia, Journal of Physics D-Applied Phys 42(2009), Article number 075306
21) M. X. Liu, B. C. Guo, Y. D. Lei, M. L. Du and D. M. Jia, Applied Surface Science 255 (2009), 4961-4969
22) M. X. Liu, B. C. Guo, Q. L. Zou, M. L. Du and D. Jia, Nanotechnology 19(2008), Article number 205709
23) Y. Q. He, W. N. Kong, W. C. Wang, T. L. Liu, Y. Liu, Q. J. Gong and J. P. Gao, Carbohydrate Polymers 87(2012), 2706-2711
24) H. Schmitt, N. Creton, K. Prashantha, J. Soulestin, M. F. Lacrampe and P. Krawczak, Polymer Engineering and Science 55 (2015) (3), 573-580
25) H. Schmitt, N. Creton, K. Prashantha, J. Soulestin, M. F. Lacrampe and P. Krawczak, Journal of Applied Polymer Science 132(2015), Article number 41341
26) H. Schmitt, K. Prashantha, J. Soulestin, M. F. Lacrampe and P. Krawczak, Carbohydrate Polymers 89 (2012), 920-927
27) M. Liu, B. Guo, M. Du and D. Jia, Applied Physics A-Materials Science & Processing 88(2007), 391-395
28) K. Y. Qiu and A. N. Netravali, Polymer Composites 34 (2013), 799-809
29) K. Y. Qiu and A. N. Netravali, Journal of Polymers and the Environment 21(2013), 658-674
30) Y. Dong, T. Bickford, H. J. Haroosh, K. T. Lau and H. Takagi, Applied Physics A-Materials Science & Processing 112 (2013), 747-757
31) H. J. Haroosh, D. S. Chaudhary and Y. Dong, Journal of Applied Polymer Science 124 (2012), 3930-3939
32) H. J. Haroosh, Y. Dong, D. S. Chaudhary, G. D. Ingram and S. Yusa, Applied Physics A-Materials Science & Processing 110 (2013), 433-442
33) Y. Dong, D. Chaudhary, H. Haroosh and T. Bickford, Journal of Materials Science 46 (2011), 6148-6153
34) K. Fujii, A. N. Nakagaito, H. Takagi and D. Yonekura, Compos Interface 21(2014), 319-327
35) H. Yano, J. Sugiyama, A. N. Nakagaito, M. Nogi, T. Matsuura, M. Hikita and K. Handa, Advanced Materials 17(2005), 153-155

(Received December, 5, 2018; Accepted January, 28, 2019)